Energetic electron avalanches and mode transitions in planar inductively coupled radio-frequency driven plasmas operated in oxygen

Zaka-ul-Islam, M., Niemi, K., Gans, T., & O'Connell, D. (2011). Energetic electron avalanches and mode transitions in planar inductively coupled radio-frequency driven plasmas operated in oxygen. Applied Physics Letters, 99(4), 041501. [041501]. DOI: 10.1063/1.3612914

Published in:
Applied Physics Letters

Energetic electron avalanches and mode transitions in planar inductively coupled radio-frequency driven plasmas operated in oxygen

M. Zaka-ul-Islam,[1,a)] K. Niemi,[1] T. Gans,[1,2] and D. O'Connell[1,2]
[1]*Centre for Plasma Physics, School of Mathematics and Physics, Queen's University Belfast, University Road, Belfast BT7 1NN, Northern Ireland, United Kingdom*
[2]*York Plasma Institute, Department of Physics, University of York, Innovation Way, Heslington York YO10 5DQ, United Kingdom*

(Received 15 March 2011; accepted 21 June 2011; published online 25 July 2011)

Space and phase resolved optical emission spectroscopic measurements reveal that in certain parameter regimes, inductively coupled radio-frequency driven plasmas exhibit three distinct operation modes. At low powers, the plasma operates as an alpha-mode capacitively coupled plasma driven through the dynamics of the plasma boundary sheath potential in front of the antenna. At high powers, the plasma operates in inductive mode sustained through induced electric fields due to the time varying currents and associated magnetic fields from the antenna. At intermediate powers, close to the often observed capacitive to inductive (E-H) transition regime, energetic electron avalanches are identified to play a significant role in plasma sustainment, similar to gamma-mode capacitively coupled plasmas. These energetic electrons traverse the whole plasma gap, potentially influencing plasma surface interactions as exploited in technological applications. © *2011 American Institute of Physics*. [doi:10.1063/1.3612914]

Low pressure high density inductively coupled plasmas (ICPs) are the core of many technological processes. It is well known that ICPs can operate in two very distinct modes: a capacitively coupled (E) mode, characterized with low plasma densities and relatively high sheath voltages and an inductively coupled (H) mode, with high densities and low sheath voltages.[1] The parameter space between both modes is often exploited for technological applications.[2]

The particular characteristics in the transition regime allow improved control over plasma parameters such as density and sheath potential, motivating applications from particle growth[3] and plasma sterilization[4] to micro-electronics processes.[5,6] However, despite the vast number of applications operating in this regime, there is still a lack of fundamental understanding. In particular, the E-H transition regime is very susceptible to instabilities. Under certain conditions, instabilities and pattern formation can occur and be detrimental to process output. With increasing demands from plasma technology, there is an urgent need to understand the underlying mechanisms of this regime and these formations.[7]

Vertical feature profiles are created through anisotropic plasma etching supported by positive ions accelerated to the substrate. During the etch process, electrons strike the side wall due to their random thermal motion. This can result in negative charging of the etch feature walls and positive charging of the bottom, leading to increased side wall etching compared to the bottom, and thus, non-ideal etch profiles. It has been shown that damage caused through charging could be highly reduced by a high-energy electron beam for neutralization of the bottom of the etch trench.[8,9] Watanabe *et al.*[8] produced this additional electron beam using a cold cathode beam source in a cylindrical ICP etcher. We illustrate that within a certain parameter regime such a high-energy electron beam may be produced in a planar ICP without the need for modification of the ICP design.

At comparatively low powers and low densities, the discharge operates in E-mode, where the antenna acts as an electrode. At increased powers, the electron density increases and the discharge can operate in H-mode when the density is high enough to sustain the induced currents. The transition from capacitive mode to inductive mode is known as the E-H transition. This can often be identified by noticeable changes in luminosity, current, and charge particle densities in the plasma.[10] Different non-linear processes have been studied during the transition such as discharge current,[10] metastable densities,[11] and influence of the external matching network.[12] Most studies have been carried out in rare gases, of little technological relevance.[10–12] In the present study, we use oxygen, a gas widely used in technical processes yet still a relatively simple electronegative molecular gas. In a certain parameter regime, we found ICPs to operate in three different operational modes, in terms of excitation processes. At comparatively low powers, the plasma is sustained through the sheath expansion dynamics. At high powers (above 280 W) the discharge is sustained in inductive mode. We see an additional excitation mechanism at intermediate powers within E-mode which is typically not considered. This shows a characteristic change of the E-mode, from alpha-mode plasma sheath heating, to a so-called gamma-like regime of capacitively coupled plasmas (CCPs)[13] where highly energetic electron avalanches traverse the discharge gap. The γ regime operates with much higher electron densities as has been reported before in CCPs.[13] This regime with high energy electrons has the potential to influence plasma surface interactions, such as avoiding charge buildup in microtrenches,[8,9] leading to improvement of the process. From a fundamental viewpoint,

a)Author to whom correspondence should be addressed. Electronic mail: mzakaulislam01@qub.ac.uk.

these high-energy electrons can also contribute to the transition from E-mode to H-mode through enhancing the plasma density. Spatio-temporal structures of high-energy electrons traversing the discharge gap were also observed in the E-mode of an ICP operated in hydrogen at higher pressure of 60 Pa (Ref. 18). The role of these electrons in the E-H transition under those conditions is not discussed in Ref. 18, however it can be expected that they play a similar role as in our experiments in oxygen at lower pressures.

The experimental setup is a standard inductively coupled Gaseous Electronics Conference (GEC) reference cell, driven at a radio-frequency of 13.56 MHz, with a planar antenna coil configuration. The plasma power is measured on the power supply as the difference between forward and reflected power. All measurements were performed at 40 Pa. Further details of the design can be found elsewhere.[14] The RF power is coupled into the plasma through a dielectric quartz window such that the plasma is not in direct contact with the antenna. The oscillating currents in the antenna generate a time dependent magnetic field inducing an electric field in the plasma. In E-mode, the antenna can also induce capacitive coupling through acting as an electrode.

The transition from the capacitive to inductive mode is investigated using phase resolved optical emission spectroscopy (PROES). PROES provides a non-intrusive access to the plasma power coupling mechanisms with excellent spatial and temporal resolution on a nanosecond time scale. This modern diagnostic technique allows investigation of the electron dynamics within the RF cycle, important for understanding the power coupling mechanisms in the discharge. Emission from the oxygen 844 nm emission line (O $(3p^3P \text{ -> } 3s^3S)$) with a lifetime of 35.1 ns, is detected using a special, fast, gate-able, intensified CCD camera (PicoStar, LaVision). An interference spectral filter is used to select the wavelength; it combines relatively high transmission and 2- dimensional spatial resolution. The bandwidth of the filter is 10 nm at full width at half maximum (FWHM). Light is collected from the region below the antenna with the camera synchronized to the RF generator, and measurements are performed with a 2 ns gate width. Phase resolved measurements over the entire RF cycle (74 ns) were obtained using a variable delay between the camera gate and the RF trigger that could be varied in increments of 2 ns. For each phase measurement, the emission was integrated over several million RF cycles to obtain an adequate signal to noise ratio. The extremely high repetition rate of the camera accepts sequential RF-cycles for integration allowing high signal-to-noise ratio. This high signal to noise ratio is required to obtain the excitation function. The high sensitivity allows changes of much less than a percent to be distinguished, translating to a temporal resolution of the order of 2 ns for the corresponding 35.1 ns lifetime of the 844 nm emission line.[15] The temporal modulation of the emission reflects the dynamics of electrons with energies greater than the excitation threshold of the observed excited state (O $(3p^3P \text{ -> } 3s^3S)$) of 10.98 eV.

Electron impact excitation out of the ground state can be described by the excitation function $E_i(t)$. The excitation function $E_i(t)$ can be determined from the measured number of photons per unit volume and unit time $\dot{n}_{ph,i}(t)$.

$$E_i(t) = \frac{1}{A_{ik} n_o} \left(\frac{d\dot{n}_{ph,i}(t)}{dt} + A_i \dot{n}_{ph,i}(t) \right)$$

where $\dot{n}_{ph,i}(t) = A_{ik} n_i(t)$ is given by the transition probability A_{ik} of the observed emission and the population density of the investigated state $n_i(t)$ and n_0 is the ground state density.[16] The effective decay rate A_i takes into account spontaneous emission, radiation trapping, and quenching.[15]

$$A_i = \sum_k A_{ik} g_{ik} + \sum_q k_q n_q$$

where g_{ik} is the so-called escape factor and k_q the quenching coefficient with the species q of density n_q. Under our conditions, the observed 844 nm emission line is optically thin $(g_{ik} = 1)$ and collisional quenching is dominated by molecular oxygen, with a quenching coefficient of $k_{O2} = 9.4 \pm 0.5 \times 10^{-10} cm^3 s^{-1}$.[17]

It is possible to distinguish between E and H-mode from the intensity[10] and temporal behavior of the emission.[18] In

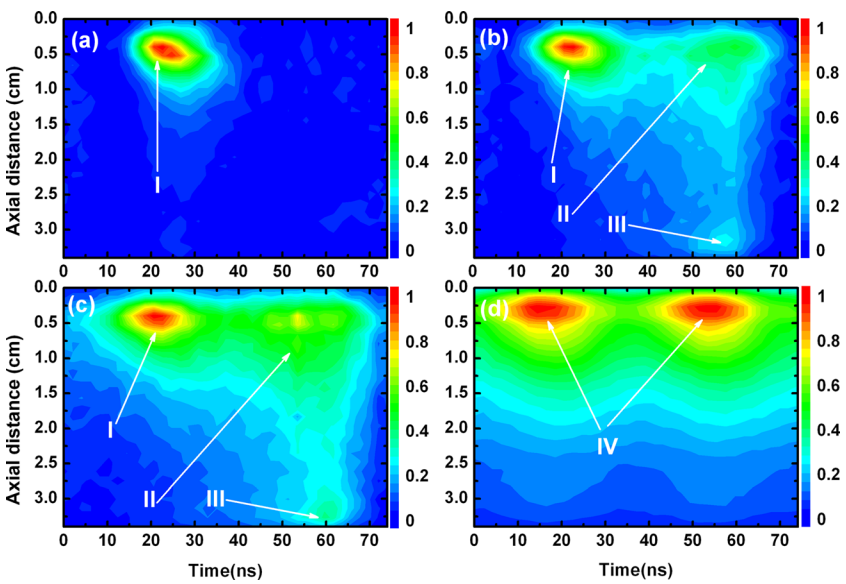

FIG. 1. (Color online) Axial time resolved excitation of the 844 nm line within one RF cycle at 40 Pa. (a) 50 W "(enhanced online, Video 1)" [URL: http://dx.doi.org/10.1063/1.3612914.1] (b) 150 W "(enhanced online, Video 2)" [URL: http://dx.doi.org/10.1063/1.3612914.2] (c) 250 W "(enhanced online, Video 3)" [URL: http://dx.doi.org/10.1063/1.3612914.3] (d) 350 W "(enhanced online, Video 4)" [URL: http://dx.doi.org/10.1063/1.3612914.4]. The printed figures show contours of temporal excitation functions in the radial center with 1-d spatial resolution along the discharge axis. 2-d spatially resolved temporal excitation functions are available online as movies corresponding to each figure.

capacitive mode, the RF dynamics is characterized by one dominant excitation per RF cycle due to sheath expansion[19] while in inductive mode, it is characterized by two excitation maxima within one cycle. This is because in inductive mode, the electron current moves clockwise in one half cycle and anti-clockwise in the other half cycle, parallel to the antenna coil.

Figures 1(a)–1(c) show the spatio-temporal plots of the excitation within one RF-cycle, at 50 W, 150 W, and 250 W, respectively, in capacitive mode. The horizontal axis shows the time of one RF cycle. The vertical axis shows the optically accessible axial distance, where the quartz plate is 0.5 cm above the $y = 0$ cm position in the plots.

Figure 1(a) shows the spatio-temporal excitation at a relatively low power of 50 W. The excitation clearly exhibits one excitation structure starting at ~15 ns. This excitation mechanism illustrates sheath expansion and is responsible for plasma sustainment at low powers.[15] This is since at low powers, the antenna acts as an electrode and electrons are accelerated perpendicularly away from the electrode once during each RF cycle. **I** denotes this excitation structure caused by sheath expansion in Figures 1(a)–1(c).

Figure 1(d) shows excitation in inductive mode at 350 W. In inductive mode, we see two similar excitations in one cycle denoted by **IV**. The inductive coupling **IV** in Figure 1(d) is attributed in the following manor. The temporal modulation of the optical emission is caused by a relative change of the electron energy. This change around the mean electron energy is determined by the induced electric field. The observed maxima in the optical emission correspond to the extrema of the induced current in the discharge. In pure inductive mode in Figure 1(d), the discharge current is sinusoidal and, therefore, the excitation maxima are exactly half a period apart.

Figure 1(b) shows a spatio-temporal plot of the emission at a power of 150 W. The dynamics is quite different to that of Figure 1(a). First, we observe similar sheath expansion as in Figure 1(a) denoted by **I**. At 150 W, another excitation mechanism appears at similar axial position after the sheath expansion, denoted by **II**. This excitation clearly traverses the entire plasma gap. Electrons generated within the sheath cause this excitation. These electrons generated within the sheath may be either secondary electrons emitted from the surface or detached electrons from negative ions.[20] These electrons are accelerated during the phase of high sheath potentials, after the sheath expansion. The decrease in the excitation in structure **II** with penetration depth shows that electrons have multiple energies. Only the electrons with comparatively higher energies are able to reach the other electrode. They cause an avalanche of excitation and ionization throughout the discharge gap (**II**), which illustrates their high energies. Their role in excitation increases with power and becomes comparable to excitation gernerated through sheath expansion near tranansition. Considering the higher energy threshold for electron impact ionization compared to excitation, the influence of energetic electron avalanches on plasma ionization and sustainment can be expected to be even more significant. Structure **III** shows excitation at the lower electrode apearing about half an RF cycle after the sheath expansion at the antenna (powered electrode).

Figure 1(c) shows the spatio-temporally resolved excitation at 250 W, also in capacitive mode, but very close to the transition to inductive mode. Here, the excitation structure **II**, due to fast electrons, is further enhanced compared to the corresponding excitation at 150 W. Also, we see a similar excitation structure due to sheath excitation at the antenna (powered electrode) **I** and at the ground electrode **III**. An interesting feature is that the transition to inductive mode seems to be supported by the increased density due to highly energetic electron avalanche across the discharge gap. This plays an important role in plasma sustainment, before the plasma turns into H-mode.

A GEC reference cell planer ICP has been investigated with space and phase resolved optical emission spectroscopy. Results show three distinct operation modes based on excitation mechanisms i.e., sheath expansion (α mode) at low powers, inductive coupling at high power, and fast electrons (γ mode) at intermediate powers. The superposition of α and γ mode is found before the discharge turns into inductive mode. These fast electrons cross the whole discharge gap, possibly influencing plasma surface interaction exploited for technological applications.

The authors acknowledge support from UK EPSRC through a Career Acceleration Fellowship (EP/H003797/1) and a Science and Innovation Award (EP/D06337X/1).

[1]M. Osiac, T. Schwarz-Selinger, D. O'Connell, B. Heil, Z. L. Petrovic, M. Turner, T. Gans, and U. Czarnetzki, Plasma Sources Sci. Technol. **16**, 355 (2007).
[2]M. A. Lieberman and A. J. Lichtenberg, *Principles of Plasma Discharges and Materials Processing*, 2nd ed. (Wiley, New York, 2005).
[3]M. Schulze, D. O'Connell, T. Gans, P. Awakowicz, and A. Keudell, Plasma Sources Sci. Technol. **16**, 774 (2007).
[4]T. Gans, M. Osiac, D. O'Connell, V. Kadetov, U. Czarnetzki, T. Schwarz-Selinger, H. Halfmann, and P. Awakowicz, Plasma Phys. Controlled Fusion **47**, A353 (2005).
[5]T. Makabe and Z. Petrović, *Plasma Electronics: Applications in Microelectronic Device Fabrication* (Taylor and Francis, New York, 2006).
[6]M. A. Sobolewski, J. Vac. Sci. Technol. A **24**, 1892 (2006).
[7]C. S. Corr, P. G. Steen, and W. G. Graham, Plasma Sources Sci. Technol. **12**(2), 265 (2003).
[8]M. Watanabe, D. Shaw, and G. Collins, Appl. Phys. Lett. **79**, 2698 (2001).
[9]M. Wang and M. J. Kushner, J. Appl. Phys. **107**, 023308 (2010).
[10]U. Kortshagen, N. Gibson, and J. Lawler, J. Physics D: Appl. Phys. **29**, 1224 (1996).
[11]A. Daltrini, S. Moshkalev, T. Morgan, R. Piejak, and W. G. Graham, Appl. Phys. Lett. **92**, 061504 (2008).
[12]F. Gao, S. X. Zhao, X. S. Li, and Y. N. Wang, Phys. Plasmas **17**, 103507 (2010).
[13]V. Godyak and A. Khanneh, IEEE Trans. Plasma Sci. **14**(2), 112 (1986).
[14]P. A. Miller, G. A. Hebner, K. E. Greenberg, and P. D. Pochan, J. Res. Natl. Inst. Stand. Technol. **100**(4), 427 (1995).
[15]T. Gans, D. O'Connell, V. Schulz-von der Gathen, and J. Waskoenig, Plasma Sources Sci. Technol. **19**, 034010 (2010).
[16]D. O'Connell, T. Gans, E. Semmler, and P. Awakowicz, Appl. Phys. Lett. **93**, 081502 (2008).
[17]K. Niemi, V. Schulz-von der Gathen, and H. Döbele, Plasma Sources Sci. Technol. **14**, 375 (2005).
[18]M. Abdel-Rahman, T. Gans, V. Schulz-von der Gathen, and H. F. Döbele, Plasma Sources Sci. Technol. **14**(1), 51 (2005).
[19]T. Gans, V. Schulz-von der Gathen, and H. Döbele, Europhys. Lett. **66**, 232 (2004).
[20]K. Dittmann, K. Matyash, S. Nemschokmichal, J. Meichsner, and R. Schneider, Contrib. Plasma Phys. **50**(10), 942 (2010).